



## Effect of Reynolds number on the wake of a Next-Generation High-Speed Train using CFD analysis

Mohammad Arafat<sup>1,\*</sup>, Izuan Amin Ishak<sup>1,2</sup>, Ahmad Faiz Mohammad<sup>3</sup>, Amir Khalid<sup>1</sup>, Md. Norrizam Mohmad Jaát<sup>1</sup>, Mohd Fuad Yasak<sup>1</sup>

<sup>1</sup> Faculty of Engineering Technology, Universiti Tun Hussein Onn Malaysia, Pagoh, Johor, Malaysia

<sup>2</sup> Sustainable Engineering Technology Research Centre, Universiti Tun Hussein Onn Malaysia, Pagoh, Johor, Malaysia

<sup>3</sup> Malaysia Japan International Institute of Technology, Universiti Teknologi Malaysia, Kuala Lumpur, Malaysia

### ARTICLE INFO

#### Article history:

Received 11 August 2022

Received in revised form 19 September 2022

Accepted 14 November 2022

Available online 12 January 2023

#### Keywords:

Aerodynamic; Computational fluid dynamics; Next-generation high-speed train (NG-HST); Reynolds number; Wake structure

### ABSTRACT

Improvement to the next-generation high-speed train (NG-HST) is ongoing particularly in achieving a higher operating speed. Consequently, the aerodynamic effect of the train will be more critical as it affects the development of a wake flow characterized by complex and unsteady structures. Although the effect of Reynolds number ( $Re$ ) on aerodynamic forces is negligible, its effect on the wake of NG-HSTs is unknown. In this study, the  $Re$  ranging from  $7.42 \times 10^5$  to  $1.62 \times 10^6$  was used to examine the characteristics of vortex structures, streamline distributions, velocity characteristics, and pressure characteristics in the wake region of an NG-HST. The Delayed Detached Eddy Simulation (DDES) is used as the turbulence model. In addition, the simulation results were compared with the previous wind tunnel experimental data. The results indicated no significant changes in the overall wake flow structure when  $Re$  was increased. According to power spectral density analysis, increasing the Reynolds number increased the turbulence intensity of the wake which gradually dissipated as the distance from the train increased. The findings of the study could be used to better understand the flow characteristics at the wake of NG-HSTs for future development.

## 1. Introduction

Flow structures around a high-speed train (HST) are complex and unsteady characterized by three-dimensional (3D) vortices. This involves vortex shedding and development of shear layer, flow separation, circulation, and a pair of counter-rotating streamwise vortices [1]. Additionally, high velocity is observable in the flow of the near wake zone of a high-speed train, which includes the nose, boundary layer, near wake, and far wake [2]. This is the result of streamwise vortex pair which consists of periodic unsteadiness and oscillation. At this stage, the flow moves towards the ground track and begins to extend outwards as the train moves further. Furthermore, it develops a complex and dynamic vortex structure with mutual induction and interaction with the ground [3]. The flow of the wake has significant effects on the trackside workers, passengers, and the nearest infrastructure

\* Corresponding author.

E-mail address: marafatbd@gmail.com

<https://doi.org/10.37934/cfdl.15.1.7687>

[4]. Some of the incidents were reported in [5]. Thus, understanding the characteristics and effect factors of high-speed train wakes is important.

Many factors, including train geometry [3], [6], bogie [7], ground effect [8], and train length [9], can influence the wake of a high-speed train. A comparative study among different train models (i.e. real model, semi-simplified model, and a simplified model) was conducted by Liu *et al.* [6]. The wake vortices in the real model are larger than those in the semi-simplified model, and both are much larger than those in the simplified model. However, because of the small size of the wake vortex, they suggested further research to determine the exact difference in the simplified model. A study by Wang *et al.* [8] shows that stationary and moving boundary conditions for the ground affect aerodynamic loads. Though, the rotating wheel effect is mostly limited to bogie regions, with little effect on the wake structure behind the train. According to Muld *et al.* [9], the major flow structure at the wake region does not change as the length changes, but there are some variations in frequency and wavelengths. In addition, other studies [10]–[12] investigated factors (ground and wheel boundary conditions, ground at the wake) affecting the wake structure of high-speed trains.

Although several studies on the effects of different Reynolds numbers ( $Re$ ) on aerodynamic characteristics such as aerodynamic loads and flow structures around HSTs are available in the literature, the impact of  $Re$  on the wake of the next-generation high-speed train (NG-HST) is unknown. The main distinction between HSTs and NG-HSTs is that the latter has a top speed of more than 400 km/h [13]. This speed is slightly faster than the current HSTs that are in service. Because of the unique shape of the train's wake nose, and when it runs at different speeds, there may be some unclear differences. In addition, the flow at the wake of a train includes a wide range of time and length scales, from the largest eddies to the smallest dissipative scales [14]. Nowadays, most research uses a scaled model to reduce computational costs, which results in a much lower Reynolds number than the corresponding full-scale test [15]. Besides, if the Reynolds number is large enough, the effect on the aerodynamic parameters is relatively small but it is often difficult in the scaled-model test [16]. This indicates the importance of further research into the impact of different Reynolds numbers, particularly for NG-HSTs.

The research aims to investigate the effect of the Reynolds number on the wake of an NG-HST. In this study, six different Reynolds numbers ranging from  $7.42 \times 10^5$  to  $1.62 \times 10^6$  are considered. This research investigates the wake flow structure, pressure, and velocity characteristics at various Reynolds numbers. The following is how this paper is constructed. The train model, numerical approach, computational domain, boundary conditions, meshes, grid convergence study, and validation are described in Section 2. Section 3 compares and analyses wake structures, streamlines on the end coach, velocity, and pressure in the wake zone at various Reynolds numbers. Section 4 contains the conclusion of the current investigation.

## 2. Methodology

### 2.1 Computational model

In the current study, the NG-HST was chosen for the investigation (Fig. 1). The full-scale length of the end car and middle car are 21 m and 20 m, respectively [17]. A simplified model of NG-HST is used for the simulation which consists of a leading car, a middle car, and an end car. 1/25<sup>th</sup> model scale train is employed; the lengths of the end car and the middle car are 840 mm and 800 mm, respectively, and the heights of both are 186 mm and 122 mm, respectively. The SolidWorks software is used to create a simplified version of the train based on the original design and specifications.

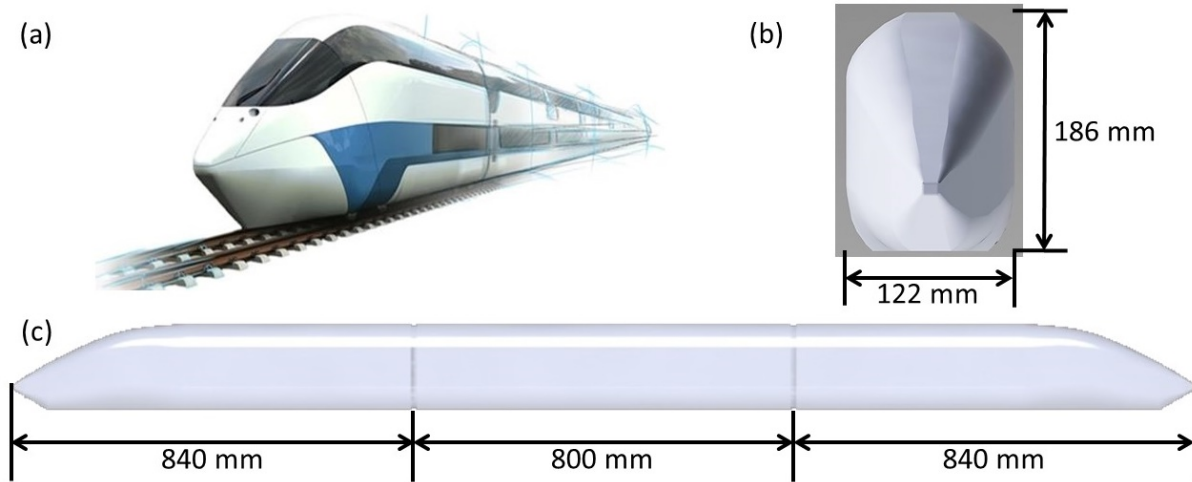


**Fig. 1.** Next Generation High-Speed Train (NG-HST) developed by German Aerospace Centre (DLR); a) NG-HST [17], b) front view, c) side view

## 2.2 Computational Boundary Condition and Domain

The computational domain of the simulation is designed to capture the flow structure at the wake of the train model. The computational domain has the following dimensions; a length of  $32H$ , a height of  $10H$ , and a width of  $16H$ , where  $H$  is the height of the train model. The domain is large enough to meet the requirements of EN14067-6:2010. The global coordinate point is at the end point of the end car. The ground surface is flat and the train has a  $0.0503$  m gap between the train and the ground; this is following the previous study [18]. This ensures that there is sufficient space between the train and the boundary conditions to prevent any unwanted interactions between them and the flow in the train's wake. The space between the train and the outlet boundary allows the wake to dissipate prior to reaching the outlet. The pressure outlet is set to zero, denoting gauge pressure as default operating pressure is  $101325$  Pa [19]. Fig. 2 displays the specifics of the boundary conditions and the domain geometry.

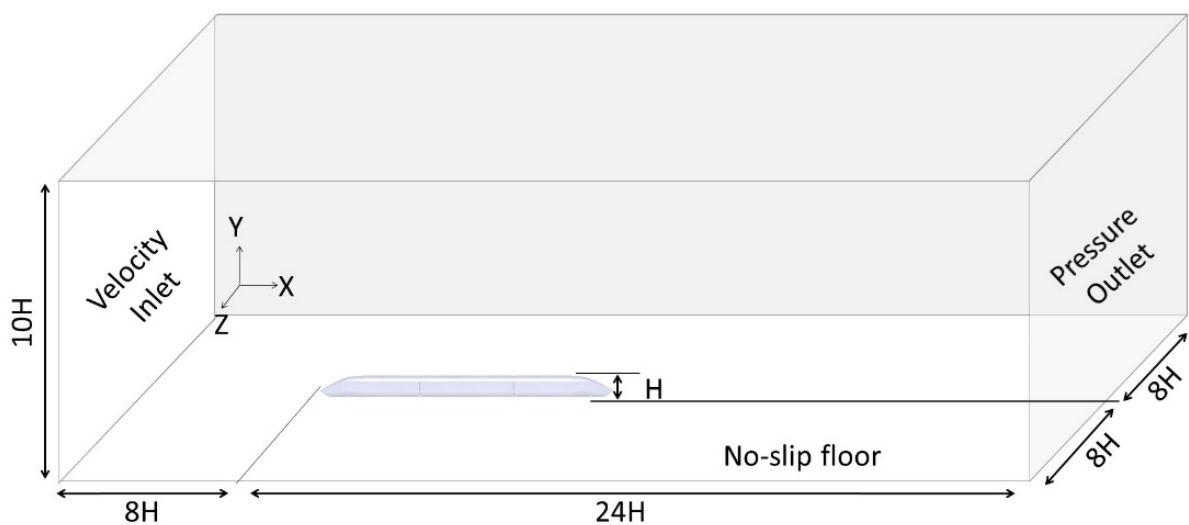


**Fig. 2.** Boundary conditions of the computational domain used in this study

The train height,  $H$  is used as the characteristic length, and thus a total of six different Reynolds numbers are used for simulating six cases based on the train height. The Reynolds numbers for the six cases are shown in Table 1. All the cases were simulated using the ANSYS Fluent software.

**Table 1**  
Six different cases of Reynolds numbers

Case 1	Case 2	Case 3	Case 4	Case 5	Case 6
$7.42 \times 10^5$	$8.7 \times 10^5$	$1 \times 10^6$	$1.16 \times 10^6$	$1.37 \times 10^6$	$1.62 \times 10^6$

### 2.3 Numerical method

The numerical simulation method used in this study is Detached Eddy Simulation (DES), which is widely used in the study of the external flow around the train. DES is one of the promising solutions proposed by Spalart in 1997 [20]. When massive separation exists, DES improves accuracy when compared to RANS, but at a lower computational cost than LES. Later, the DES technique was improved to Delayed Detached Eddy Simulation (DDES) for grid introduce separation [21]. The accuracy of turbulence prediction using various turbulence models including LES, DES, and RANS was investigated on a generic high-speed train model by Krajnović [22]. In addition, Morden et al. [23] used surface pressures of a high-speed train to compare a set of RANS and two DES models to wind tunnel data for a zero yaw angle. Their findings indicated that DDES provided highest accuracy for the aerodynamic characteristics (surface pressure) when compared to the experimental data. Therefore, in this study, the Delayed Detached Eddy Simulation (DDES) model is used. The RANS equations describe the behaviour of a fluid or flow over time. The deduction is based on Reynolds decomposition, which divides time-averaged and fluctuating variables.

Transient and time steps of 0.004 were used in this numerical simulation utilising a Shear Stress Transport or SST-based DDES turbulence model. This results in a maximum Courant number,  $Co$  of approximately unity. The COUPLED approach is applied for pressure-velocity coupling. For spatial discretization, a second-order upwind approach with a Bounded Central Differencing scheme is used.

### 2.4 Meshing method

The ANSYS Advanced Meshing module is used to generate a structured hexa-dominant mesh. Details of the mesh are displayed in Fig. 3. Two refinement boxes are employed to improve the mesh and capture flow structure around and behind the train. The dimensions ( $L \times H \times W$ ) of the two refinement boxes are  $8000 \times 450 \times 800$  mm and  $3500 \times 250 \times 300$  mm, respectively. In addition, on the train's surface, a 5-layer boundary layer mesh is constructed. The first layer thickness is 0.01 mm to keep the  $y$ -plus on the train surface within 30.

To analyse mesh sensitivity, three different mesh resolutions are considered [24]. Moreover, with the availability of wind tunnel data of the previous study [25], an NG-HST model consisting of a leading car and half of the middle car is used for the mesh independence study. The details of the difference between each of the mesh resolutions are represented in

Table 2.

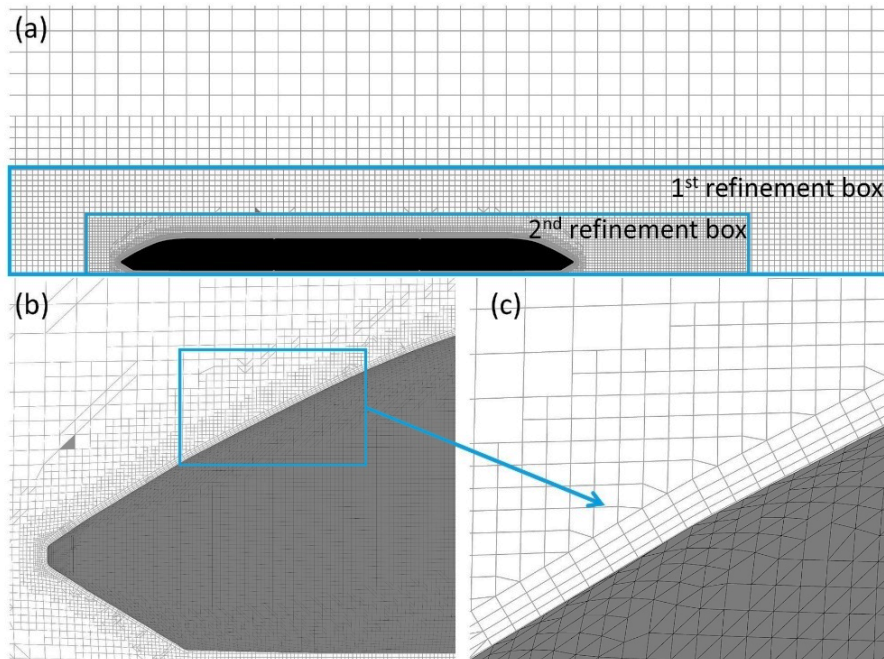


**Fig. 3.** Mesh resolution used in the case simulation; a) train model and refinement box, b) nose of the train, c) inflation layers on the train surface

**Table 2**

Three mesh resolutions with the associated parameters

Parameters	Fine (3)	Medium (2)	Coarse (1)
Face element size (mm)	0.5	1	2
Inflation layer	5	5	5
First Inflation layer height (mm)	0.25	0.50	1
1 <sup>st</sup> Refinement box element size (mm)	20	30	40
2 <sup>nd</sup> Refinement box element size (mm)	5	10	20
Total elements number, $N$	1,199,674	513,197	272,503

### 2.5 Grid Convergence Study and Validation

The drag coefficient ( $C_d$ ) is considered the main aerodynamic parameter for the grid convergence analysis in this study. It can be seen in Fig. 4 that the difference of the drag value is smaller between medium and fine meshes compared with coarse and medium meshes. This means that decreasing the mesh element size improves the prediction accuracy. The relative percentage difference between fine and medium meshes is about 0.5% while for coarse and medium around 2%. This means a further improvement in mesh quality will not have much effect on the  $C_d$ . Therefore, the fine mesh resolution is adequate for the simulation to study the flow structure by ensuring computational accuracy. Furthermore, because this research focuses on the train's wake area, extra fine mesh is required to resolve the flow structures more accurately. As a result, the mesh number in the case simulation was increased to approximately 5 million.

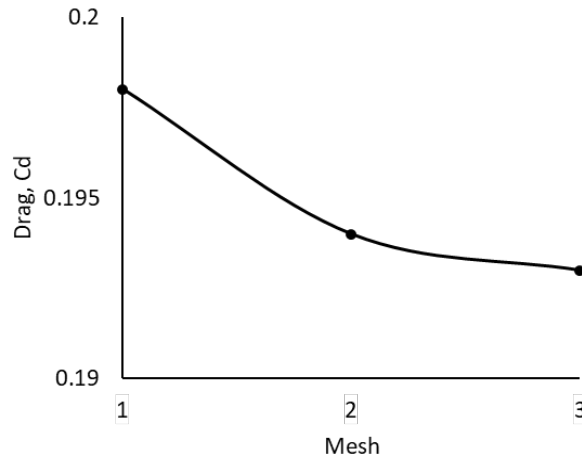


Fig. 4. Drag coefficients at different mesh resolutions

To validate the current simulation results, numerical results are compared with the wind tunnel data from the previous study as shown in Table 3. In the previous study by Fragner *et al.* [25], the RANS model was employed using OpenFOAM and DLR TAU<sup>1</sup> code. The aerodynamic coefficients in the current study are better compared with the CFD simulation results in the previous study. In addition, the relative percentage error of the  $C_d$  between experimental and current simulation work is about 7%, which is reasonable.

**Table 3**  
Comparison of experimental and simulation results

Method	Drag, $C_d$
Experiment [25]	0.18
OpenFOAM [25]	0.21
TAU [25]	0.20
Current Study (Ansys, DDES)	0.193

### 3. Results and discussion

#### 3.1 Vortex Structures and Formation

The vortex structure in the wake region of the NG-HST is analysed in this section. Six different Reynolds numbers were considered for the simulation of six cases. There are several methods available in the literature to demonstrate the structure of a three-dimensional vortex, such as the Q criterion,  $\Delta$  criterion,  $\lambda$  criterion, etc. The Q criterion is used in the current study to observe the wake vortex.

The instantaneous wake vortex of the NG-HST is shown in Fig. 5. There is a vorticity formation very close to the wake. In addition, no discernible difference is observed in the size of the vortex. That is, as the  $Re$  increases, the changes in vorticity remain nearly unchanged. The height and the width of the two main vortex cores are also the same. This differs from the study on an ICE high-speed train model conducted by [16].

<sup>1</sup>The DLR TAU code is a modern software system for the prediction of viscous and inviscid flows about complex geometries from the low subsonic to the hypersonic flow regime, employing hybrid unstructured grids composed of tetrahedrons, pyramids, prisms and hexahedrons [27].

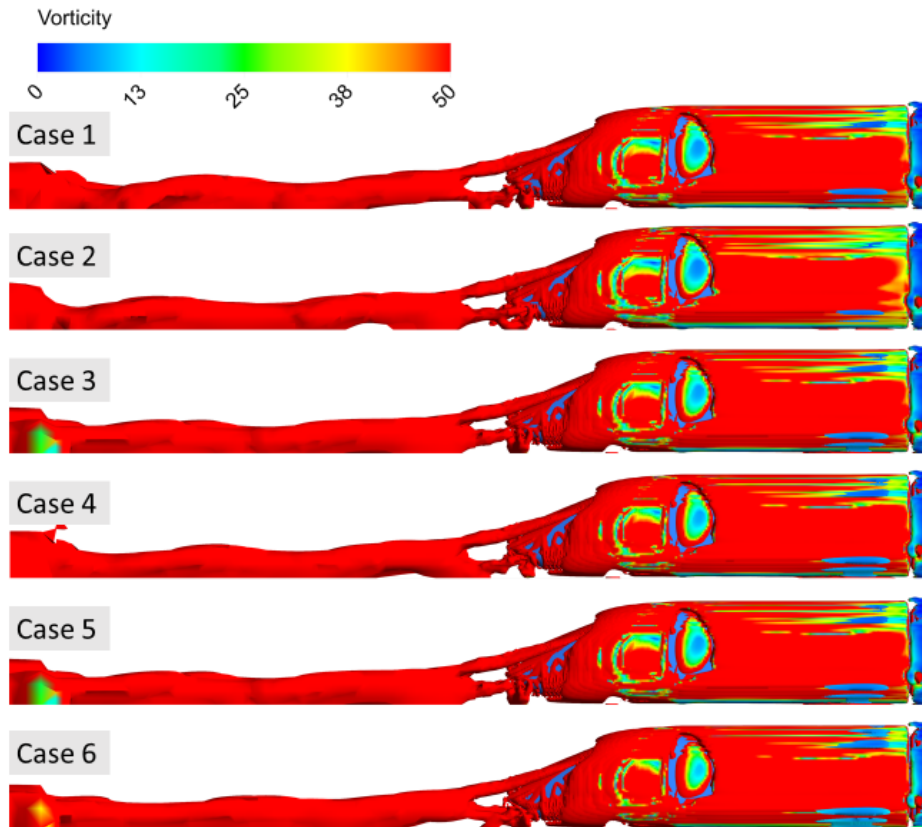


Fig. 5. Side view of the instantaneous vortex core region near the wake of the train

Furthermore, the vorticity contour and velocity vector are analysed to understand more about the wake vortex structures and behaviour. However, there are no significant differences in the  $Re$  in this case. A study by Bell *et al.* [26] shows different types of vortices formed at the wake of HSTs. Among the usual streamwise vortex characteristics at the wake that formed, there is a pair of counter-rotating vortices. Similar types of vortices at the wake of NG-HST are also observed in Fig. 6.

There are two major vortices formed at different locations of the wake, which begin at the edge of the end car and move downwards, and as the distance from the train increases, the vortices are moving outward. Additionally, it is obvious that the vortex intensity is very high near the end car and decreases when it is far from the end car due to the dissipation of the fluid's turbulent kinetic energy. The results also show that as the Reynolds number increases, so does the vertical vorticity. As a result of the high energy, the vortex becomes more intense.

Power spectral density (PSD) analysis was performed on the instantaneous velocity data in the wake of the NG-HST at different  $Re$ . A velocity measuring point is chosen for this analysis at the wake region at  $x = 1H$ ,  $y = -0.25H$ ,  $z = 0.12H$ .

PSD of the velocity which is based on the dimensionless Strouhal number ( $St$ ) at the velocity measuring point is shown in Fig. 7. PSD of the lowest and highest  $Re$  shows the frequency of the velocity where the major frequency of the velocity recorded is between 0.2 and 0.3. Furthermore, the dominant frequency of the velocity is found to be nearly the same for other Reynolds numbers. However, as the  $Re$  increases, the vortex intensity of the wake motion becomes more noticeable. According to Han *et al.* [16], frequency characteristics of the velocity at the end car region reflect the vortex shedding of the wake. This means that the vortex shedding should be the same regardless of the  $Re$ . According to the current findings, the vortex at the wake is nearly identical.

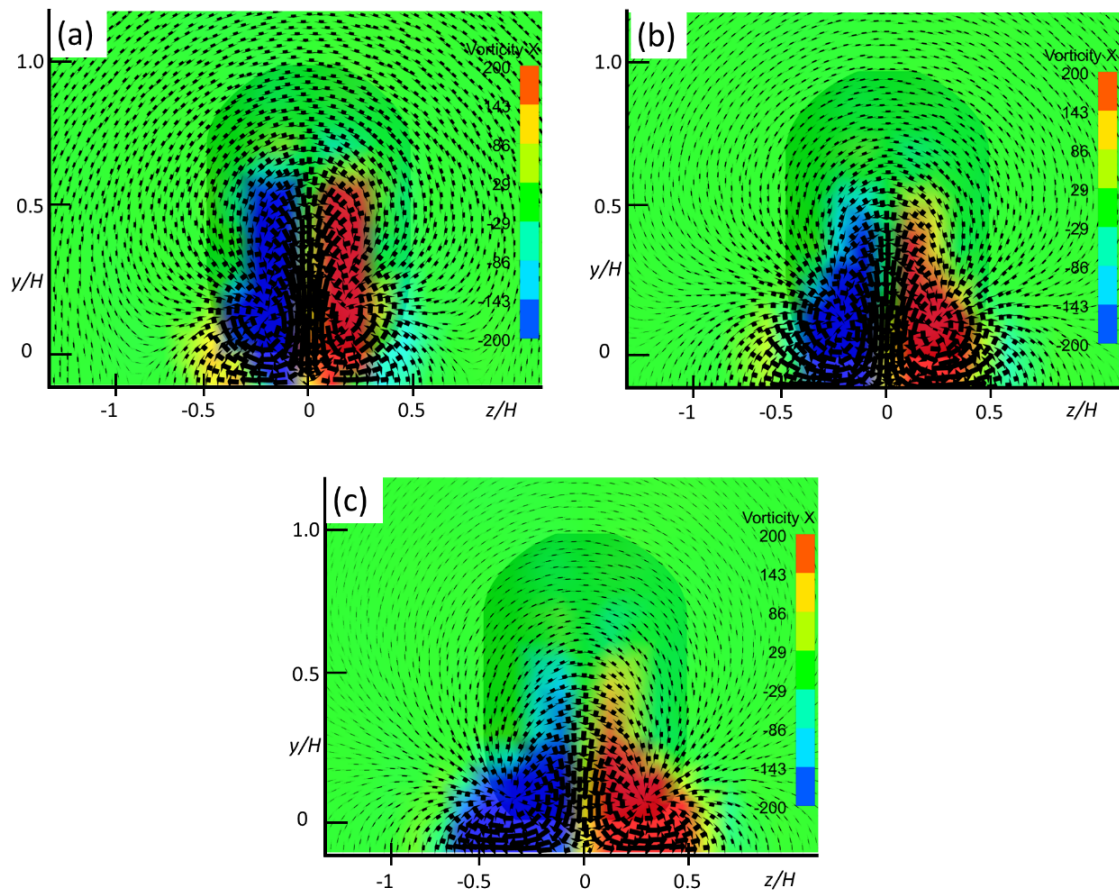


**Fig. 6.** Velocity vectors and vorticity ( $\omega_x$ ) contour; a)  $Re = 1.62 \times 10^6$  at  $x=1H$ ; b)  $Re = 7.42 \times 10^5$  at  $x = 2H$ ; c)  $Re = 1.16 \times 10^6$  at  $x = 4H$

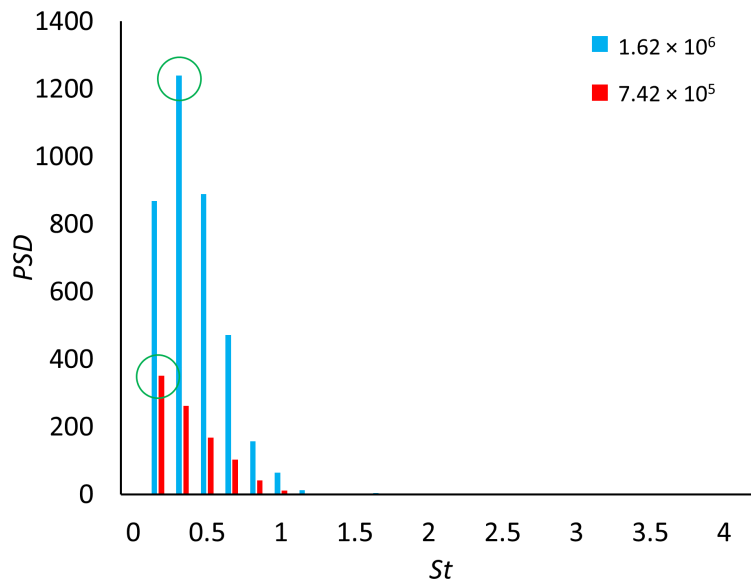


**Fig. 7.** Power spectral density of velocity at point  $(x = 1H, y = -0.25H, z = 0.12H)$

### 3.2 Streamlines and Velocity Characteristics

This section discusses streamlines on the train surface and slipstream velocity characteristics. Vortex shedding and wake flow structures are induced by flow separation on the train surface. Streamlines on the train surface at varying values of the  $Re$  are shown in Fig. 8.

All cases with different  $Re$  values show that the separation line at the end car of the train formed on both sides. In addition, vortices can be seen at the bottom of the nose tip. That is, the streamwise vortices visible in Fig. 6 are the result of the separated lines on the end car. This can also explain the presence of vortices on the bottom of the end car's nose tip in Fig. 5. It is therefore possible to conclude that there is a relationship between flow separation on the end car and the wake flow structure characteristics.

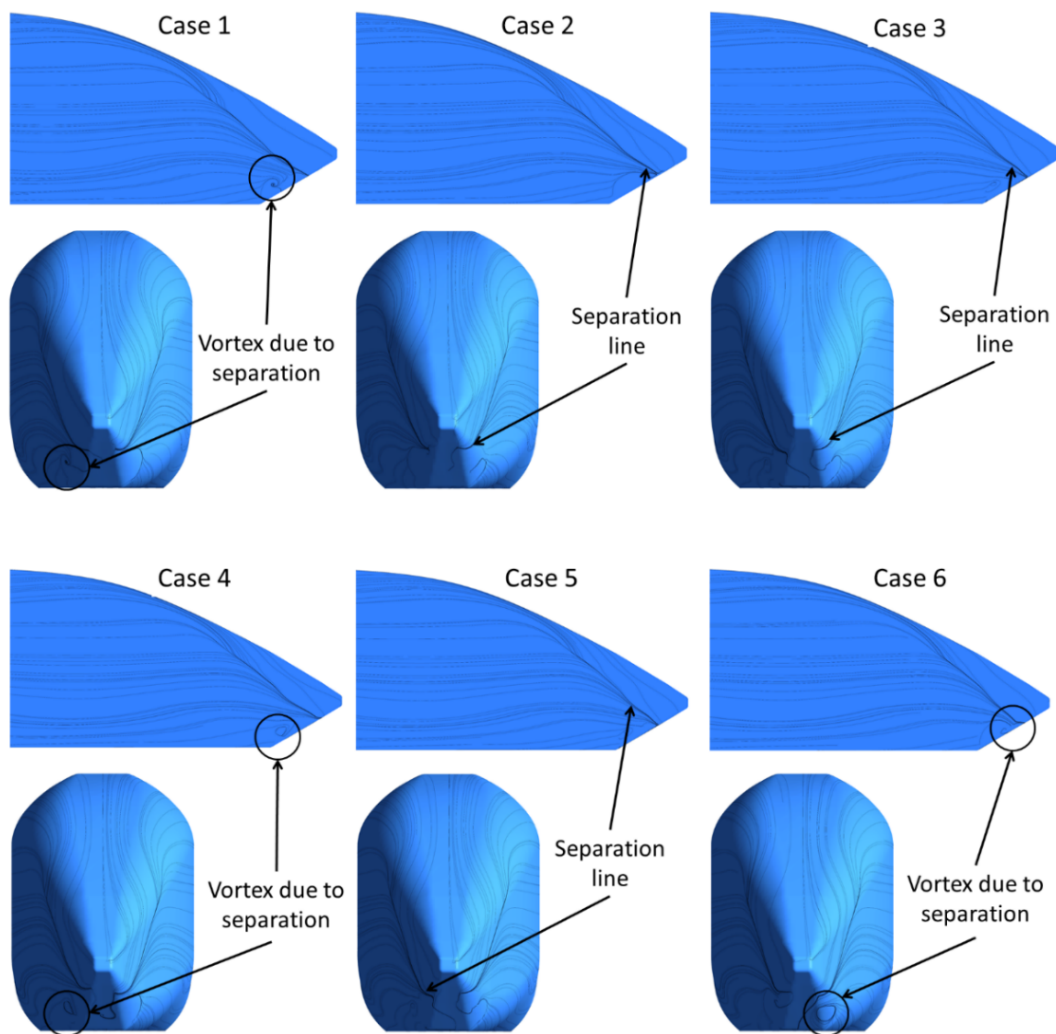


**Fig. 8.** Wake surface streamlines for different cases

Slipstream velocity contour along with the streamlines on the wake of the NG-HST is presented in Fig. 9. The figure shows the formation of vortices on both sides of the end car. There is no significant difference except for cases 4 and 6. With respect to the different  $Re$ , the changes in the flow behavior and flow separation remained the same. Thus, there is no effects of Reynolds numbers on the slipstream flow characteristics in the wake of NG-HST.

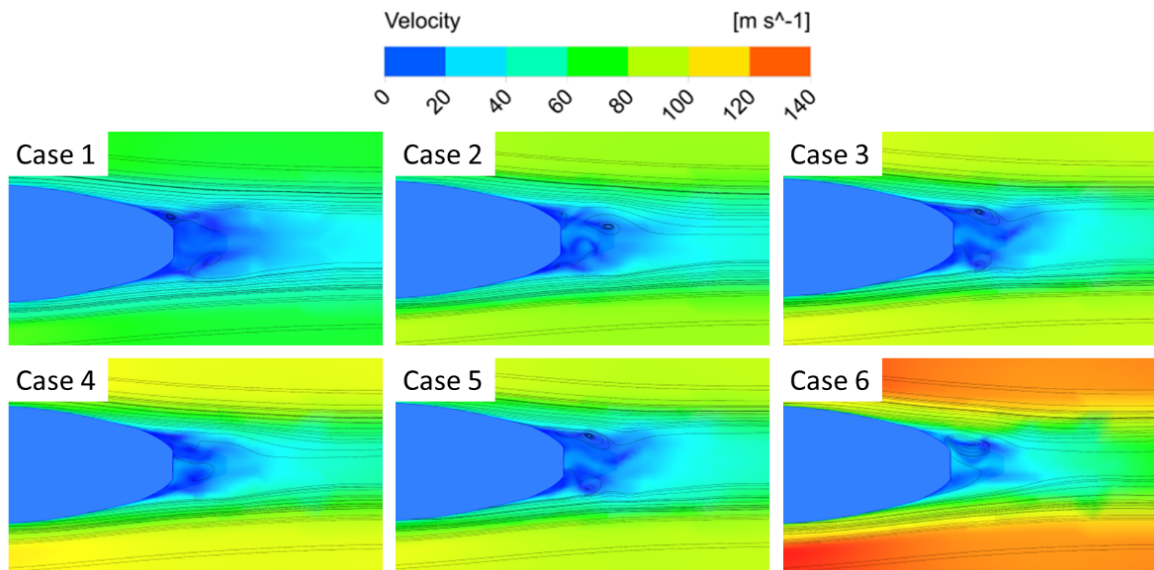


Fig. 9. Slipstream velocity along with the streamlines at  $y = -0.4H$

### 3.3 Pressure distribution and characteristics

A contour of pressure coefficient in different Reynolds numbers at the wake is shown in Fig. 10 to understand the pressure distribution. All of the cases show a spanwise vortex that expands as the train moves forward. Vortices exhibit both positive and negative pressures symmetrically at the near and far wake of the train.

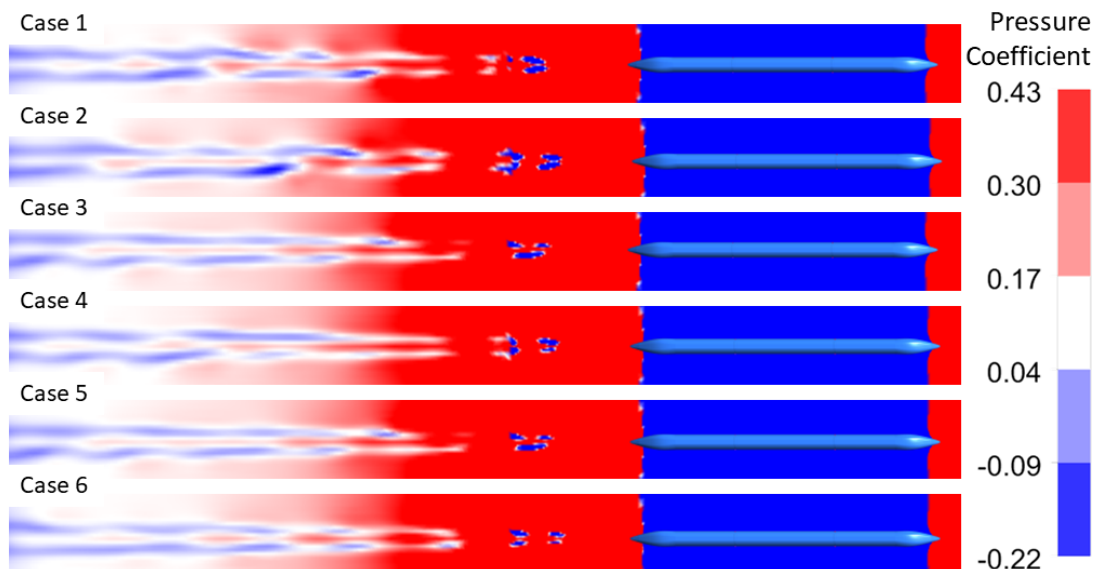


Fig. 10. Top view of the pressure coefficient contours for different Reynolds numbers

The pressure characteristics change insignificantly as the Reynolds number increases. As a result, there are no significant effects of  $Re$  on the pressure distribution.

## 4. Conclusion

The current work investigated the effects of different Reynolds numbers on the wake of a simplified model of an NG-HST. The Reynolds number ranging from  $7.42 \times 10^5$  to  $1.62 \times 10^6$  was used to investigate the detailed flow structures including wake vortices, surface streamlines, and streamwise velocity vectors, as well as to examine power spectral density analysis and pressure distribution.

According to the simulation results, there were no significant changes in the overall flow structure in the wake of NG-HST. As a result, it can be concluded that the Reynolds number has no significant effect on the flow structure in the wake region. The authors are aware of the analysis procedure used to produce the results; if not due to grid size (one of the limitations of the current study), there could be another reason, – i.e., unique shape of the NG-HST, which is originally designed and optimised by DLR to achieve low energy consumption and aerodynamic shape. According to the power spectral density analysis, increasing the Reynolds number increased the turbulent intensity. Furthermore, the intensity of the vortex decreases as the distance from the end car increases.

Furthermore, vortices near the end car may affect the dynamic performance of the NG-HST, which is directly related to the train operational safety. As part of the current project, the dynamic analysis will be performed in the future study.

## Acknowledgment

This research was financially supported by the Malaysia Ministry of Higher Education (MOHE) through Fundamental Research Grant Scheme (FRGS/1/2020/TK02/UTHM/03/4).

## References

- [1] Bell, J. R., D. Burton, M. C. Thompson, A. H. Herbst, and J. Sheridan. "Dynamics of trailing vortices in the wake of a generic high-speed train." *Journal of Fluids and Structures* 65 (2016): 238-256. <https://doi.org/10.1016/j.jfluidstructs.2016.06.003>
- [2] Sterling, Mark, C. J. Baker, S. C. Jordan, and T. Johnson. "A study of the slipstreams of high-speed passenger trains and freight trains." *Proceedings of the Institution of Mechanical Engineers, Part F: Journal of Rail and Rapid Transit* 222, no. 2 (2008): 177-193. <https://doi.org/10.1243/09544097JRR133>
- [3] Bell, J. R., D. Burton, M. C. Thompson, Astrid H. Herbst, and J. Sheridan. "The effect of tail geometry on the slipstream and unsteady wake structure of high-speed trains." *Experimental Thermal and Fluid Science* 83 (2017): 215-230. <https://doi.org/10.1016/j.expthermflusci.2017.01.014>
- [4] Ishak, Izuan Amin, Mohamed Sukri Mat Ali, Mohamad Fitri Mohd Yakub, and Sheikh Ahmad Zaki Shaikh Salim. "Effect of crosswinds on aerodynamic characteristics around a generic train model." *International Journal of Rail Transportation* 7, no. 1 (2019): 23-54. <https://doi.org/10.1080/23248378.2018.1424573>
- [5] Figura-Hardy, G. I. "RSSB Slipstream Safety-Analysis of existing experimental data on train slipstreams including the effects on pushchairs." *Rail Safety and Standards Board*(2007).
- [6] Liu, Wen, Dilong Guo, Zijian Zhang, Dawei Chen, and Guowei Yang. "Effects of bogies on the wake flow of a high-speed train." *Applied Sciences* 9, no. 4 (2019): 759. <https://doi.org/10.3390/app9040759>
- [7] Jiang, Zhiwei, Tanghong Liu, Houyu Gu, and Zijian Guo. "A numerical study of aerodynamic characteristics of a high-speed train with different rail models under crosswind." *Proceedings of the Institution of Mechanical Engineers, Part F: Journal of Rail and Rapid Transit* 235, no. 7 (2021): 840-853. <https://doi.org/10.1177/0954409720969250>
- [8] Wang, Shibo, David Burton, Astrid H. Herbst, John Sheridan, and Mark C. Thompson. "The effect of the ground condition on high-speed train slipstream." *Journal of Wind Engineering and Industrial Aerodynamics* 172 (2018): 230-243. <https://doi.org/10.1016/j.jweia.2017.11.009>
- [9] Muld, Tomas W., Gunilla Efraimsson, and Dan S. Henningson. "Wake characteristics of high-speed trains with different lengths." *Proceedings of the Institution of Mechanical Engineers, Part F: Journal of Rail and Rapid Transit* 228, no. 4 (2014): 333-342. <https://doi.org/10.1177/0954409712473922>
- [10] Zhang, Jie, Jing-juan Li, Hong-qi Tian, Guang-jun Gao, and John Sheridan. "Impact of ground and wheel boundary conditions on numerical simulation of the high-speed train aerodynamic performance." *Journal of Fluids and*

- Structures61 (2016): 249-261. <https://doi.org/10.1016/j.jfluidstructs.2015.10.006>
- [11] Xia, Chao, Hanfeng Wang, Xizhuang Shan, Zhigang Yang, and Qiliang Li. "Effects of ground configurations on the slipstream and near wake of a high-speed train." *Journal of Wind Engineering and Industrial Aerodynamics* 168 (2017): 177-189. <https://doi.org/10.1016/j.jweia.2017.06.005>
- [12] Xia, Chao, Hanfeng Wang, Di Bao, and Zhigang Yang. "Unsteady flow structures in the wake of a high-speed train." *Experimental Thermal and Fluid Science* 98 (2018): 381-396. <https://doi.org/10.1016/j.expthermflusci.2018.06.010>
- [13] Arafat, Mohammad, and Izuan Amin Ishak. "CFD Analysis of the Flow around Simplified Next-Generation Train Subjected to Crosswinds at Low Yaw Angles." *CFD Letters* 14, no. 3 (2022): 129-139. <https://doi.org/10.37934/cfdl.14.3.129139>
- [14] Muld, Tomas W. "Analysis of flow structures in wake flows for train aerodynamics." PhD diss., 2010.
- [15] Li, Tian, Hassan Hemida, Jiye Zhang, Mohammad Rashidi, and Dominic Flynn. "Comparisons of shear stress transport and detached eddy simulations of the flow around trains." *Journal of Fluids Engineering* 140, no. 11 (2018). <https://doi.org/10.1115/1.4040672>
- [16] Y. Han, D. Chen, S. Liu, and G. Xu, "An investigation into the effects of the Reynolds number on high-speed trains using a low temperature wind tunnel test facility," *Fluid Dyn. Mater. Process.*, 16, no. 1 (2020): 1–19. <https://doi.org/10.32604/fdmp.2020.06525>
- [17] Winter, Joachim. "Novel rail vehicle concepts for a high speed train: the next generation train." In *Proceedings of the First International Conference on Railway Technology: Research, Development, Maintenance*. Civil-Comp Press, 2012.
- [18] Wang, Shuangbu, Ruibin Wang, Yu Xia, Zhenye Sun, Lihua You, and Jianjun Zhang. "Multi-objective aerodynamic optimization of high-speed train heads based on the PDE parametric modeling." *Structural and Multidisciplinary Optimization* 64, no. 3 (2021): 1285-1304. <https://doi.org/10.1007/s00158-021-02916-0>
- [19] L. W. Chen, I. A. Ishak, M. Arafat, N. Farhan, N. A. Samiran, and A. F. Mohammad, "Analysis of the Aerodynamic Characteristics of Small-Sized Car Vehicles under the Influence of Steady Crosswind," in *International Conference on Applied Science, Technology, and Engineering (ICASTE)*, 2022.
- [20] Spalart, Philippe R. "Comments on the feasibility of LES for wings, and on a hybrid RANS/LES approach." In *Proceedings of first AFOSR international conference on DNS/LES*. Greyden Press, 1997.
- [21] Spalart, Philippe R., Shur Deck, Michael L. Shur, Kyle D. Squires, M. Kh Strelets, and Andrei Travin. "A new version of detached-eddy simulation, resistant to ambiguous grid densities." *Theoretical and computational fluid dynamics* 20, no. 3 (2006): 181-195. <https://doi.org/10.1007/s00162-006-0015-0>
- [22] S. Krajnović, "Unsteady simulations in train aerodynamics," in *Civil-Comp Proceedings*, 2014, vol. 104.
- [23] Morden, Justin A., Hassan Hemida, and Chris Baker. "Comparison of RANS and detached eddy simulation results to wind-tunnel data for the surface pressures upon a class 43 high-speed train." *Journal of Fluids Engineering* 137, no. 4 (2015). <https://doi.org/10.1115/1.4029261>
- [24] Ishak, I. A., M. S. M. Ali, and SAZ Shaikh Salim. "Numerical simulation of flow around a simplified high-speed train model using OpenFOAM." In *IOP Conference Series: Materials Science and Engineering*, vol. 152, no. 1, p. 012047. IOP Publishing, 2016. <https://doi.org/10.1088/1757-899X/152/1/012047>
- [25] Fagner, Moritz M., Keith A. Weinman, Ralf Deiterding, Uwe Fey, and Claus Wagner. "Comparison of industrial and scientific CFD approaches for predicting cross wind stability of the NGT2 model train geometry." *The International Journal of Railway Technology* 4, no. 1 (2015): 1-28. <https://doi.org/10.4203/ijrt.4.1.1>
- [26] Bell, J. R., D. Burton, M. C. Thompson, A. H. Herbst, and J. Sheridan. "Dynamics of trailing vortices in the wake of a generic high-speed train." *Journal of Fluids and Structures* 65 (2016): 238-256. <https://doi.org/10.1016/j.jfluidstructs.2016.06.003>
- [27] Schwamborn, Dieter, Anthony Gardner, Heiko von Geyr, Andreas Krumbein, Heinrich Lüdeke, and Arne Stürmer. "Development of the TAU-Code for aerospace applications." (2008).